PHYSICAL REVIEW A VOLUME 16, NUMBER 5 NOVEMBER 1977

Statistical mechanics of dense ionized matter. VII. Equation of state and phase separation of ionic mixtures in a uniform background

J. P. Hansen
Laboratoire de Physique Théorique des Liquides, Université de Paris VI, 75230 Paris Cedex 05, France*

G. M. Torrie†
Laboratoire de Physique Théorique et Hautes Energies,‡ Université de Paris-Sud, 91405 Orsay, France

P. Vieillefosse
Laboratoire de Physique Théorique des Liquides, Université de Paris VI, 75230 Paris Cedex 05, France*
(Received 4 March 1977)

By solving the hypernetted chain (HNC) equation for the pair distribution functions, and by Monte Carlo simulations, we have calculated the equation of state and the pair structure of dense binary mixtures of classical point ions in a rigid, uniform background of opposite charge. All of our results indicate that the excesss internal and free energies of mixing are negligible compared to the energies of the mixture or the pure phases, for ionic-charge ratios $Z_2/Z_1 = 2$ and 3, in the strong coupling (high density or low temperature) regime. This feature allows us to write down a simple equation of state for such mixtures, which is used to determine the phase diagram of pressure-ionized H-He and H-Li mixtures in a rigid background of degenerate electrons. We then treat the polarization of the electron gas by the ionic-charge distribution by perturbation theory and include quantum corrections to the free energy of the ions. Both effects do not drastically modify the phase diagrams. The applicability of our results in astrophysical situations is discussed.

I. INTRODUCTION

In the study of the equilibrium and transport properties of dense fully ionized matter, the classical one-component plasma (OCP) has proved to be a very useful model: the ions are regarded as point charges, whereas the degenerate electron gas is assumed to form a uniform and rigid continuum (or background), ensuring overall charge neutrality. This model of fully ionized matter is also referred to as "jellium," and its applications range from astrophysics to metallic hydrogen. Since the pioneer work of Brush, Sahlin, and Teller,[1] the thermodynamic properties, equilibrium structure, and dynamical properties of the OCP have been quantitatively studied by Monte Carlo[2] and molecular-dynamics[3] computer simulations, and by the numerical solution of integral equations.[4] The present paper is devoted to an extension of the equilibrium calculations to the case where two ionic species are present, in particular H^+-He^{++} and H^+-Li^{+++} mixtures.

Stenvenson[5] has recently shown that H^+-He^{++} mixtures in a *responding* electron background phase separate under temperature and pressure conditions characteristic of the interior of Jupiter. In his calculation, Stevenson used a hard-sphere reference system and thermodynamic perturbation theory to describe the ions, and the Hubbard-Geldart-Vosko[6] dielectric function to describe the response of the electron gas. Some Monte Carlo results[7] are also available for mixtures with low-number concentrations of He ions, the linear response of the electron gas being described by the Lindhard dielectric function.[8] This paper presents the first extensive numerical results for the thermodynamic properties and equilibrium structure of two component ionic plasmas in a rigid uniform background over a wide range of temperatures, densities, and concentrations, and for the two ionic charge ratios $Z_2/Z_1 = 2$ and 3. These results lead to a very simple equation of state which is then applied to the study of the phase diagram of such mixtures. Quantum corrections and the effects of the polarization of the electron gas by the ionic charge distribution (i.e., electron screening effects) are handled by perturbation theory.

The outline of the paper is the following: The model, all relevant parameters, and some general properties are introduced in Sec. II. The results from the nonlinear Debye-Hückel theory are presented in Sec. III. Section IV contains the results from numerical solutions of the hypernetted chain (HNC) integral equation for the pair-distribution functions. Monte Carlo (MC) data are presented in Sec. V and compared to the results of Secs. III and IV. "One-fluid" models are briefly discussed in Sec. VI. The phase diagrams of H^+-He^{++} and H^+-Li^{+++} mixtures, based on the preceding results, are drawn in Sec. VII. Quantum corrections and electron screening corrections are treated in Sec. VII, while Sec. IX contains some concluding re-

marks.

A brief account of parts of this work has been published elsewhere.[9]

II. THE MODEL

Consider a mixture of N_1 ions of charge $Z_1 e$ and N_2 ions of charge $Z_2 e$ ($Z_2 > Z_1$) in a volume V; e is the elementary charge. The partial number densities are $\rho_1 = N_1/V$ and $\rho_2 = N_2/V$, the number concentrations are $x_1 = N_1/N$ and $x_2 = N_2/N = 1 - x_1$, the total number density is $\rho = \rho_1 + \rho_2 = N/V$, and the charge density (divided by e) is $\rho' = Z_1\rho_1 + Z_2\rho_2 = \langle Z\rangle_{\rm av}\rho$, where $\langle Z\rangle_{\rm av}$ is the mean charge $x_1 Z_1 + x_2 Z_2$. The uniform background charge density is of opposite sign. If the background is rigid (nonresponding) the interaction Hamiltonian for the periodic system can be cast in the form

$$H = \frac{1}{2V}{\sum_{\vec{k}}}' \frac{4\pi e^2}{k^2}(\rho'_{\vec{k}}\rho'_{-\vec{k}} - N\langle Z^2\rangle_{\rm av}), \tag{1}$$

where $\rho'_{\vec{k}}$ is a Fourier component of the charge density,

$$\rho'_{\vec{k}} = \sum_{i=1}^{N} Z_i e^{i\vec{k}\cdot\vec{r}_i}; \tag{2}$$

$\langle Z^2\rangle_{\rm av} = x_1 Z_1^2 + x_2 Z_2^2$, and the prime in the summation means that the term $\vec{k} = 0$ is left out, to take proper account of the uniform background.

We define the "ion-sphere" radius $a = (3/4\pi\rho)^{1/3}$ and the "electron-sphere" radius $a' = (3/4\pi\rho')^{1/3} = a/\langle Z\rangle_{\rm av}^{1/3}$. Apart from the ideal gas contributions, the thermodynamic state of the ionic mixture is completely determined by x_1 and the dimensionless coupling parameter

$$\Gamma = e^2/ak_B T, \tag{3}$$

where T is the temperature. Alternatively, we can choose as independent variables x_1 and

$$\Gamma' = e^2/a'k_B T = \Gamma\langle Z\rangle_{\rm av}^{1/3}. \tag{4}$$

In the density and temperature range that will be considered here, the Fermi temperature of the electrons $T_F \gg T$, so that the electron gas is completely degenerate and is entirely characterized by the usual dimensionless length parameter:

$$r_s = a'/a_0, \tag{5}$$

where a_0 is the electronic Bohr radius. If we consider moreover the limit $r_s \ll 1$, the electron gas is completely rigid and does not affect the ion-ion interaction, which is then given correctly by (1). We shall call this simplified model of an ionic mixture the "two-component plasma" (TCP) by analogy with its one-component counterpart, the OCP. The equilibrium properties of the classical TCP will be studied in Secs. III–VII, while the more realistic case taking due account of quantum effects and the polarization of the electron background by the ionic charge distribution, will be considered in Sec. VIII.

In the following we choose a as the unit of length and use dimensionless Fourier transforms:

$$\hat{f}(q) = 3\int_0^\infty \frac{\sin qx}{qx} f(x)x^2\,dx, \tag{6}$$

where $x = r/a$, $q = ka$, and $4\pi\rho a^3 = 3$. Let $g_{\nu\mu}(x)$ be the partial-pair-distribution functions ($\nu, \mu = 1, 2$), $h_{\nu\mu}(x) = g_{\nu\mu}(x) - 1$ the pair-correlation function, and $c_{\nu\mu}(x)$ the direct-correlation functions, which are related to the $h_{\nu\mu}$ by the Ornstein-Zernike equations:

$$\hat{h}_{\nu\mu}(q) = \hat{c}_{\nu\mu}(q) + \sum_{\alpha=1}^{2} x_\alpha \hat{h}_{\nu\alpha}(q)\hat{c}_{\alpha\mu}(q). \tag{7}$$

Let $\rho_{\vec{q}}^{(\nu)}$ be the Fourier components of the partial-number densities:

$$\rho_{\vec{q}}^{(\nu)} = \sum_{i=1}^{N_\nu} e^{i\vec{q}\cdot\vec{r}_i} \quad (\nu = 1, 2). \tag{8}$$

The partial-structure factors are then defined as

$$S_{\nu\mu}(q) = (N_\nu N_\mu)^{-1/2}\langle \rho_{\vec{q}}^{(\nu)}\rho_{-\vec{q}}^{(\mu)}\rangle = \delta_{\nu\mu} + (x_\nu x_\mu)^{1/2}\hat{h}_{\nu\mu}(q). \tag{9}$$

A quantity of central importance is the charge-density structure factor

$$S'(q) = \frac{1}{N\langle Z^2\rangle_{\rm av}}\langle \rho'_{\vec{q}}\rho'_{-\vec{q}}\rangle = \frac{1}{N\langle Z^2\rangle_{\rm av}}\sum_\nu\sum_\mu (x_\nu x_\mu)^{1/2} \times Z_\nu Z_\mu[\delta_{\nu\mu} + (x_\nu x_\mu)^{1/2}\hat{h}_{\nu\mu}(q)]. \tag{10}$$

Comparing (1) and (10), we see that the excess (nonideal) internal energy of the TCP can be expressed in terms of $S'(q)$ through

$$u = \frac{\beta U^{\rm ex}}{N} = \frac{\Gamma\langle Z^2\rangle_{\rm av}}{\pi}\int_0^\infty [S'(q) - 1]\,dq, \tag{11}$$

and, using the virial theorem, the equation of state then follows from

$$\beta PV/N = 1 + \tfrac{1}{3}u, \tag{12}$$

where $\beta = 1/k_B T$.

The usual charge-neutrality and perfect-screening conditions[10] imply that

$$S'(q) \underset{q\to 0}{\simeq} q^2/3\Gamma\langle Z^2\rangle_{\rm av}. \tag{13}$$

A straightforward fluctuation calculation, along the lines of a similar calculation in Ref. 11 for the OCP, or in Ref. 12 for a binary molten salt, yields the following expression for $S'(q)$, which becomes exact in the long-wavelength limit ($q \to 0$):

$$S'(q) = [(3\Gamma\langle Z^2\rangle_{\rm av}/q^2)(1-\delta q^2)]^{-1},$$

$$\delta = -\frac{1}{3\Gamma\langle Z\rangle_{\rm av}}\left[\beta\left(\frac{\partial P}{\partial \rho'}\right)_{T,x_1} - \frac{\langle Z\rangle_{\rm av}^3}{\langle Z^2\rangle_{\rm av}} x_1 x_2 \frac{[(\beta/\rho')(\partial P/\partial x_1)_{\rho',T}]^2}{1+(\langle Z\rangle_{\rm av} x_1 x_2/\langle Z^2\rangle_{\rm av})[(\partial/\partial x_1)\langle Z\rangle_{\rm av}^2(\partial/\partial x_1)\beta F/N']_{\rho',T}}\right], \tag{14}$$

where F is the Helmoholtz free energy, $N' = \bar{Z}N$ is the total number of charges, and T, ρ', and x_1 were chosen as independent variables.

The isothermal compressibility χ_T can be expressed in terms of the direct-correlation functions through a suitable generalization of the compressibility equation[13]:

$$\frac{\chi_T^0}{\chi_T} = \left(\frac{\partial \beta P}{\partial \rho}\right)_{T,x_1}$$

$$= x_1\left(\frac{\partial \beta P}{\partial \rho_1}\right)_{T,\rho_2} + x_2\left(\frac{\partial \beta P}{\partial \rho_2}\right)_{T,\rho_1}$$

$$= 1 - \lim_{q\to 0}\left[\sum_\nu\sum_\mu x_\nu x_\mu\left(\hat{c}_{\nu\mu}(q) + \frac{3\Gamma Z_\nu Z_\mu}{q^2}\right)\right], \tag{15}$$

where $\chi_T^0 = \beta/\rho$ is the isothermal compressibility of an ideal gas, taken at the same temperature and density.

In the weak-coupling limit ($\Gamma \ll 1$), the excess internal energy tends towards its Debye-Hückel (DH) limit

$$u^{\rm DH} = -\tfrac{1}{2}\sqrt{3}\,(\Gamma\langle Z^2\rangle_{\rm av})^{3/2}. \tag{16}$$

Mermin[14] has shown that (16) yields a lower bound to u for any value of Γ. In the DH limit we also have

$$\hat{c}_{\nu\mu}^{\rm DH}(q) = -3\Gamma Z_\nu Z_\mu/q^2. \tag{17}$$

In the strong-coupling limit ($\Gamma' \gg 1$) we expect u to approach its value calculated in the framework of the "ion-sphere" (IS) model.[15] In this model, each ion interacts only with the uniform background in its "ion sphere," i.e., a sphere of radius $a_\nu/a = (Z_\nu/\bar{Z})^{1/3}$ such that the background charge contained in it exactly cancels the charge Z_ν of the ion. An elementary calculation then yields

$$u^{\rm IS} = -0.9\Gamma\langle Z\rangle_{\rm av}^{1/3}\langle Z^{5/3}\rangle_{\rm av} = -0.9\Gamma'\langle Z^{5/3}\rangle_{\rm av}. \tag{18}$$

In fact, by a straightforward generalization of a proof by Lieb and Narnhofer[16] for the OCP, it can be shown that (18) also yields a lower bound to u for all Γ. It is interesting to compare the lower bounds (16) and (18); for a given value of x_1, the two bounds are equal when

$$\Gamma = \Gamma_0 = \tfrac{27}{25}\,(\langle Z\rangle_{\rm av}^{1/3}\langle Z^{5/3}\rangle_{\rm av}/\langle Z^2\rangle_{\rm av})^2, \tag{19}$$

which is of order 1, except for very large charge ratios Z_2/Z_1. When $\Gamma < \Gamma_0$, $u^{\rm DH} > u^{\rm IS}$, i.e., $u^{\rm DH}$ is closer to the exact energy; the converse is true for $\Gamma > \Gamma_0$. Thus we anticipate two rather different regimes; for $\Gamma < \Gamma_0$, we expect the dimensionless thermodynamic properties to behave roughly as their DH limits, whereas for $\Gamma > \Gamma_0$, we expect these properties to be essentially linear in Γ.

For sufficiently strong coupling, we expect the TCP to crystallize, just as the OCP does.[2] In fact, the internal energy (18) of the ion sphere model is very close to the ionic energies calculated for a number of ionic compounds on cubic lattices.[17] Although we shall briefly return to the question of crystallization in Sec. VI, the bulk of this paper will be devoted to the fluid phase of ionic mixtures, with special emphasis on two-component systems with charge ratios $Z_2/Z_1 = 2$ and 3.

III. NONLINEAR DEBYE-HÜCKEL THEORY

We have first calculated the pair-correlation functions and the equation of state of the TCP in the framework of the nonlinearized version of Debye-Hückel theory, i.e., by solving the complete coupled Poisson-Boltzmann equations numerically.[15] In the limit $\Gamma \to 0$, the nonlinear DH theory reduces of course to its linearized form. On the other hand it can be easily shown from the Poisson-Boltzmann equations that the internal energy satisfies the inequality

$$u \geq -\tfrac{3}{4}\Gamma'\langle Z^{5/3}\rangle_{\rm av}. \tag{20}$$

This is of the same form as the exact bound (18), except for the numerical factor. Numerical solutions for various values of x_1 and Z_2/Z_1, indicates that for $\Gamma' > 1$ (strong coupling), the calculated internal energy tends rapidly towards its lower bound [Eq. (20)].

In Table I we compare the internal energies of the linear and nonlinear DH theories, with the more accurate predictions of HNC theory (cf. Sec. IV). As expected the linear DH results differ quite sensibly already for $\Gamma = 0.1$, whereas the nonlinear DH and the HNC results are in excellent agreement at that Γ, and are still reasonably close at $\Gamma = 1$. Since the HNC results will be shown to be in excellent agreement with the "exact" Monte Carlo results (see Sec. V), we conclude that the nonlinear DH theory is surprisingly accurate up to $\Gamma \simeq 1$, and not unreasonable for even stronger couplings.

TABLE I. Comparison between excess internal energies u calculated in the linear and nonlinear Debye-Hückel approximations, and in the HNC approximation for ionic mixtures with $Z_1=1$, $Z_2=2$.

Γ	x_1	HNC	Nonlinear DH	Linear DH
0.1	1	−0.02568	−0.025591	−0.027386
	0.75	−0.0557	−0.055207	−0.063399
	0.5	−0.0914	−0.090198	−0.108253
	0.25	−0.1316	−0.129552	−0.160456
	0	−0.1759	−0.172641	−0.219089
1	1	−0.5705	−0.54846	−0.866025
	0.75	−1.075	−1.01296	−2.00488
	0.5	−1.639	−1.52872	−3.42327
	0.25	−2.253	−2.08790	−5.07406
	0	−2.911	−2.68493	−6.92820

A final feature which appears from inspection of Table II is that u, calculated in the nonlinear DH approximation, is nearly *linear* in x_1 for fixed Γ', in agreement with the lower bound [Eq. (20)] which is exactly linear in x_1. This behavior will be confirmed by the HNC and MC results.

IV. HNC SOLUTIONS FOR THE TCP

Recent careful calculations by Springer *et al.* and by Ng[4] and the comparison with "exact" Monte Carlo computations[4,18] show that among the usual integral equations for the pair distribution functions,[19] the HNC approximation gives by far the best results for the one component plasma as it does for long-range potentials in general. In fact the internal energy of the OCP calculated in the HNC approximation differs by less than 1% from the MC results for all Γ. It is reasonable to expect a similar situation for ionic mixtures, and the purpose of this and Sec. V is to show that this is indeed the case.

The perfect screening condition[10] implies that the direct-correlation functions behave like the corresponding pair potentials for large interionic distances; more precisely,

$$c_{\nu\mu}(x) \underset{x\to\infty}{\longrightarrow} -\beta v_{\nu\mu}(x) = -Z_\nu Z_\mu \Gamma/x\,. \tag{21}$$

Consequently, we define short-range direct-correlation functions

$$c^s_{\nu\mu}(x) = c_{\nu\mu}(x) + Z_\nu Z_\mu \Gamma/x\,, \tag{22}$$

whose Fourier transform is regular in the limit $q\to 0$. The HNC approximation for the pair-distribution functions $g_{\nu\mu}$ then reads

$$g_{\nu\mu}(x) = \exp[h_{\nu\mu}(x) - c^s_{\nu\mu}(x)]\,. \tag{23}$$

Equation (23) together with the Ornstein-Zernike relations (7) form a closed set of three integral equations for the $g_{\nu\mu}$ which we have solved iteratively using a generalization of the procedure described by Ng[4] in the case of the OCP. The internal energy and the pressure were then calculated via Eqs. (11) and (12). The excess (nonideal) Helmholtz free energy can be calculated either by integrating the internal energy with respect to Γ for a fixed value of x_1:

$$f(\Gamma,x_1) = \frac{\beta F^{\rm ex}}{N}(\Gamma;x_1) = \int_0^\Gamma u(\gamma,x_1)\frac{d\gamma}{\gamma}\,, \tag{24}$$

or directly from the excess chemical potentials which are given, in the framework of the HNC approximation, by the following formula:

$$\beta\mu^{\rm ex}_\nu = \sum_{\mu=1}^{2} x_\mu \left(\frac{3}{2}\int_0^\infty h_{\nu\mu}(x) \times [h_{\nu\mu}(x) - c_{\nu\mu}(x)]x^2\,dx - \hat{c}^s_{\nu\mu}(0) \right). \tag{25}$$

Equation (25) is a generalization of a formula derived by Verlet and Levesque[20] in the case of simple liquids; a proof is given in Appendix A, but it must be kept in mind that such relations, which express chemical potentials in terms of pair-correlation functions, hold only within the HNC approximation. In that framework the free energies derived from (24) and (25) are consistent and the agreement between the numerical values obtained through the two different channels serves only as a check on the numerical accuracy of the compu-

TABLE II. Excess internal energy u and excess internal energy of mixing Δu [cf. Eq. (27)] calculated in the nonlinear DH approximation for $\Gamma'=0.1$ and three values of Z_2 ($Z_1=1$).

	$Z_2=2$		$Z_2=3$		$Z_2=10$	
x_1	$-u$	Δu	$-u$	Δu	$-u$	Δu
1	0.025591	0	0.025591	0	0.025591	0
0.75	0.049818	0.001161	0.091922	0.003787	0.784789	0.023266
0.5	0.075117	0.001251	0.162185	0.003642	1.572612	0.017908
0.25	0.100968	0.000788	0.233808	0.002138	2.363544	0.009440
0	0.127145	0	0.306064	0	3.155449	0

tations.

The situation is quite different for the isothermal compressibility, which can be calculated either via (15), or by differentiating the internal energy with respect to Γ for fixed x_1:

$$\chi_T^0/\chi_T = 1 + \tfrac{1}{9}\left[\Gamma(\partial u/\partial\Gamma) + 3u\right]_{x_1} . \tag{26}$$

The two routes to the compressibility are *not* automatically consistent, since they lead to identical results only if the *exact* pair correlation functions are used in (11) and (15).

We have solved the HNC equations for two charge ratios: $Z_2/Z_1 = 2$ and 3; three concentrations: $x_1 = 0.25$, 0.5, and 0.75; and for several values of Γ, in the range $0.05 \leq \Gamma \leq 80$. From our discussion in Sec. VI it will become clear that we have covered practically the entire fluid range of the TCP. Our numerical procedure and the convergence of the iterative scheme are sufficient to ensure five significant figures on our energy values.

A comparison of these values with the energies calculated for the OCP in the HNC approximation,[4] i.e., the energies for $x_1 = 0$ and 1, shows that for a fixed value of the coupling parameter Γ', $u(\Gamma', x_1)$ is remarkably *linear* in the concentrations. In other words all our results indicate that the excess internal energy of mixing at constant Γ' (i.e., constant temperature and charge density),

$$\Delta u(\Gamma', x_1) = u(\Gamma', x_1) - x_1 u(\Gamma', x_1 = 1) - x_2 u(\Gamma', x_2 = 1), \tag{27}$$

is negligible compared to $u(\Gamma', x_1)$. If $u_0(\Gamma) = (\beta U_0^{ex}/N)(\Gamma)$ is the excess internal energy of the OCP, as a function of Γ, Eq. (27) can be rewritten

$$u(\Gamma', x_1) \simeq x_1 u_0(\Gamma' Z_1^{5/3}) + x_2 u_0(\Gamma' Z_2^{5/3}) , \tag{28}$$

i.e., the equation of state of the TCP can be expressed very simply in terms of the known equation of state of the OCP. More precisely, $\Delta u(\Gamma', x_1)$ appears to be always *positive*, but very small; for $Z_2/Z_1 = 2$, our numerical results indicate that $\Delta u \lesssim 0.005$ for all Γ; this represents about 0.3% of u at $\Gamma' \simeq 1$, and less than 0.01% at $\Gamma' = 40$. In fact, for fixed x_1, Δu is roughly independent of Γ' for $\Gamma' \gtrsim 1$, and its relative importance decreases rapidly, since u increases approximately linearly with Γ'. Only in the limit $\Gamma' \ll 1$ does Δu become a sizable fraction of the energy of the mixture.

In the strong-coupling limit, the calculated internal energies approach rather closely their lower bound (18). The difference is of the order of 3% for $\Gamma' = 50$. Note that the lower bound (18) exactly satisfies equation (27).

For the ratio $Z_2/Z_1 = 3$, we reach similar conclusions, except that in this more asymmetric case, the excess energy of mixing is slightly larger, as one would intuitively expect; we find that $\Delta u \gtrsim 0.01$ in this case, which is still practically negligible compared to u, except when $\Gamma' \ll 1$.

If we neglect Δu, the equation of state of the TCP reduces to the very simple form (28). u_0 is well known,[4] and the HNC results have been fitted very accurately by De Witt,[18] who has proposed a simple functional form valid for $\Gamma > 1$. We prefer to use a fit which is slightly less accurate, but which has the advantage of going over to the correct DH limit when $\Gamma \to 0$:

$$u_0(\Gamma) = \Gamma^{3/2}\left[A_1/(B_1 + \Gamma)^{1/2} + A_2/(B_2 + \Gamma)\right] , \tag{29}$$

where $A_1 = -0.899\,962$, $B_1 = 0.702\,482$, $A_2 = 0.274\,105$, and $B_2 = 1.319\,505$. The equation of state of the TCP follows from replacing (29) in (28). All other thermodynamic properties can now be derived from (28) via (12), (24), and (26); the excess specific heat at constant volume follows from

$$c_v = \frac{C_v}{Nk_B} = -\Gamma'^2 \frac{\partial}{\partial\Gamma'}\left(\frac{u}{\Gamma'}\right)_{x_1} . \tag{30}$$

It is worth mentioning that careful numerical integration of our energy data leads to excess Helmholtz free energies of mixing which are slightly larger than the excess internal energies of mixing; we find

$$0 \leq \Delta f(\Gamma', x_1) \lesssim 0.03 \quad \text{for } Z_2/Z_1 = 2 , \qquad 0 \leq \Delta f(\Gamma', x_1) \lesssim 0.05 \quad \text{for } Z_2/Z_1 = 3 . \tag{31}$$

These values are still negligible for most practical purposes.

A serious difficulty arises when we consider the values of the isothermal compressibilities obtained either via (15) or via (26). As indicated earlier we do not expect the two expressions to yield the same values in the HNC approximation. In fact we find that the two routes yield inverse compressibilities which differ by as much as 30% at large Γ'! The situation is pictured in Fig. 1, where we have plotted both estimates of χ_T^0/χ_T as a function of Γ for $x_1 = 0.5$ and $Z_2/Z_1 = 2$. The large discrepancy is the consequence of an internal inconsistency of the HNC approximation, and is not unlike the well-known difference between the "virial" and "compressibility" equations of state of a hard-sphere fluid as obtained in the Percus-Yevick approximation.[19] The same discrepancy exists in the case of the HNC results for the OCP, but had not been pointed out before. Because of this serious inconsistency, we cannot *a priori* trust the HNC results, and "exact" Monte Carlo calculations have to be carried out to check the

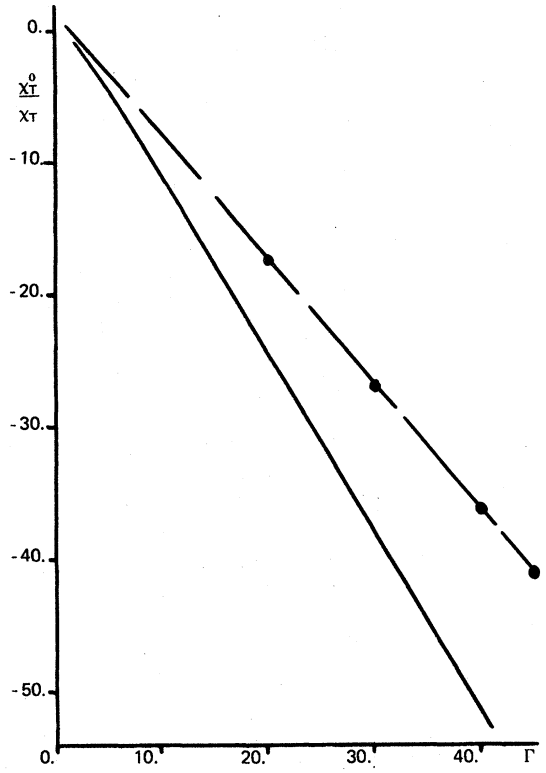

FIG. 1. Inverse compressibility χ_T^0/χ_T as a function of Γ; full curve: HNC result based on the compressibility equation (15); dashed line: HNC result based on differentiation of the equation of state; dots: MC results.

accuracy of the HNC equation of state (see Sec. V). Both estimates of the compressibility show that χ_T^0/χ_T becomes *negative* for $\Gamma' \gtrsim 1$, just as in the case of the OCP.[2] It has been shown however that this feature entails no fundamental difficulty.[11]

An example of the three pair-distribution functions $g_{\nu\mu}(x)$ is shown in Fig. 2 and compared to the MC results. As expected $g_{22}(x)$ (corresponding to the higher charge species) shows more structure than $g_{12}(x)$ and $g_{11}(x)$. Contrary to the nonlinear DH result, the $g_{\nu\mu}(x)$ exhibit oscillations, characteristic of short-range order, above some critical value of Γ' (of order unity) for a given value of x_1. The $c_{\nu\mu}^s(x)$'s, defined by (22) are very-short-ranged functions; beyond $x \simeq 2$ all three are practically zero. The full direct-correlation functions $c_{\nu\mu}(x)$ have a behavior qualitatively similar to that of $c(x)$ for the OCP [cf. Fig. 3 of Ref. 2(a)].

V. MONTE CARLO RESULTS

In order to check our HNC results and, in particular, the validity of (28), we have carried out Monte Carlo computer "experiments" for a TCP with ionic charge $Z_1 = 1$ and $Z_2 = 2$, for a range of Γ values and three concentrations. The MC program used in Ref. 2 needed only slight modifications to be adapted to the two component case, and we refer the reader to that paper for technical details, particularly the treatment of the long range of the Coulomb potential under periodic boundary conditions by Ewald summation techniques.

The first $(0.5-1)\times 10^5$ configurations of each run were discarded and the internal energy and pair distribution function averaged over a further $(2-4)\times 10^5$ configurations. The results for the internal energy of seven different (Γ, x) states of a 128-ion system are summarized in Table III where they are compared with the HNC results. In calculating Δu we have used the MC results for the OCP given in Ref. 2. In order to estimate the N dependence of the MC energies, we repeated three runs for a system of 250 ions and these results are also displayed in Table III. Since the estimated statistical uncertainty in u is of the order of ± 0.01, the differences between the $N = 128$ and $N = 250$ results are well within the combined uncertainties, and we are therefore confident that the quoted energy values are close to their thermodynamic limit.

Inspection of Table III shows that the "exact" MC energies are systematically lower than their HNC counterparts, though the relative difference is al-

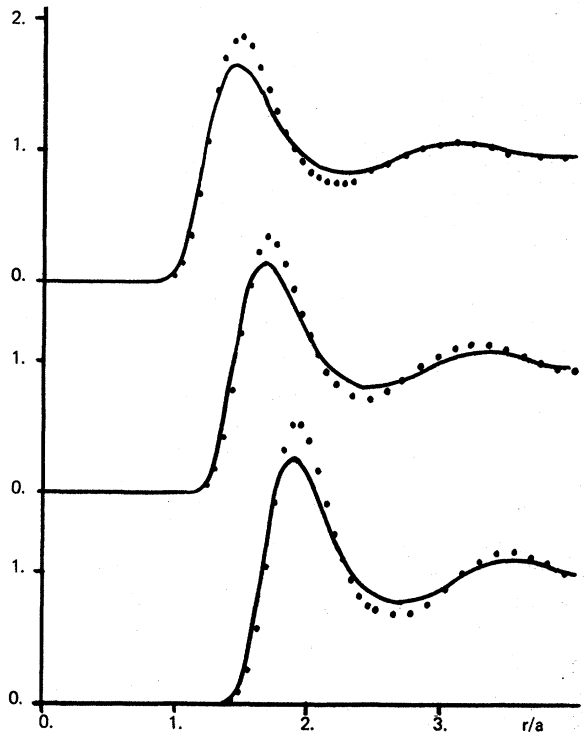

FIG. 2. From top to bottom: $g_{11}(x)$, $g_{12}(x)$, and $g_{22}(x)$ as a function of $x = r/a$, for an ionic mixture $Z_1 = 1$, $Z_2 = 2$, at $\Gamma = 40$, $x_1 = 0.5$; full curves: HNC results; dots: MC results.

TABLE III. Comparison between Monte Carlo and HNC results for the excess internal energy u and the excess energy of mixing Δu [cf. Eq. (27)], for ionic mixtures with $Z_1=1$ and $Z_2=2$. N is the number of particles used in the MC simulations.

		MC			HNC	
Γ	x_1	N	$-u$	Δu	$-u$	Δu
1	0.5	128	1.651	0.002	1.639	0.005
1	0.5	250	1.645	0.008		
5	0.5	128	9.715	0.000	9.638	0.004
10	0.75	128	13.777	−0.002	13.670	0.003
10	0.5	128	20.134	−0.010	19.975	0.005
10	0.25	128	26.964	−0.001	26.771	0.004
10	0.248	250	27.016	0.004	26.828	0.004
20	0.5	128	41.201	−0.004	40.919	0.004
20	0.5	250	41.191	0.006		
40	0.5	128	83.643	−0.024	83.161	0.004

ways less than 1%; a similar situation holds for the OCP. In view of the statistical uncertainties in the MC data, the excess energy of mixing cannot be determined with the precision of the HNC results; according to the latter, Δu is positive and always less than 0.005, which is below the statistical noise level of the MC results. Bearing this in mind, the value $\Delta u=0$ for all Γ and x_1 would be compatible with the MC data quoted in Table III. If we adopt this value, the "exact" equation of state of the TCP reduces to (28), where $u_0(\Gamma)$ is now the "exact" internal energy of the OCP.[2] This has been fitted as a simple function of Γ, by DeWitt[18]

$$u_0(\Gamma)=a\Gamma+b\Gamma^{1/4}+c\,. \tag{32}$$

The best fit of the MC energy data over the range $1\lesssim\Gamma\lesssim 160$ is achieved with $a=-0.896\,434$, $b=0.86185$, $c=-0.5551$. The corresponding excess free-energy function is

$$f_0(\Gamma)=a\Gamma+4b\Gamma^{1/4}+c\ln\Gamma+d\,, \tag{33}$$

with $d=-2.996$. The isothermal compressibility obtained by differentiating the internal energy via (26) is in good agreement with the HNC compressibility obtained in a similar fashion, as shown in Fig. 1 for equal concentrations of the ions. Since the pair correlation functions obtained by the MC method are "exact," the compressibility calculated through (15) agrees with its value obtained via (26), except for numerical inaccuracies due to statistical errors.

Figure 2 shows the three pair-distribution functions at $\Gamma=40$, $x_1=0.5$, from the MC and HNC calculations. The MC $g_{\nu\mu}(x)$'s are seen to exhibit a more pronounced structure than their HNC counterparts. The excellent agreement between the MC and HNC internal energies, despite the appreciable quantitative differences that occur for the pair functions, is the result of cancellation of positive and negative errors in the short-range part of the HNC pair functions. This is a quite general feature for both the TCP and the OCP.

VI. "ONE-FLUID" MODELS

Although we now have at our disposal a very accurate equation of state of the TCP, it is interesting to see whether one can formulate a simple van der Waals "one-fluid theory" of ionic mixtures in terms of the properties of the OCP, and some "effective" charge Z_e. Such theories have been moderately successful in the description of simple liquid mixtures of components which are not too dissimilar.[21] The main problem lies in finding a simple recipe for determining Z_e. In terms of Z_e, the interaction Hamiltonian of the one-component reference system reads

$$H_0=\frac{1}{2V}{\sum_{\vec{k}}}'\frac{4\pi(Z_e)^2}{k^2}(\rho_{\vec{k}}\rho_{-\vec{k}}-N)\,, \tag{34}$$

where $N=N_1+N_2$ is the total number of ions of charge Z_e and $\rho_{\vec{k}}=\rho_{\vec{k}}^{(1)}+\rho_{\vec{k}}^{(2)}$. If we consider $H-H_0$ [where H is given by (1)] as a perturbation, we know from the Gibbs-Bogoliubov inequality that the sum of the zeroth- and first-order terms of thermodynamic perturbation theory yield an *upper* bound to the excess Helmholtz free energy of the TCP for any choice of Z_e (Ref. 21):

$$f(\Gamma,x_1)\le f_0(\Gamma Z_e^2)+(\beta/N)\langle H-H_0\rangle_0\,, \tag{35}$$

where the statistical average of $H-H_0$ is taken over the reference system canonical ensemble. Equation (41) is easily transformed into

$$f(\Gamma,x_1)\le f_0(\Gamma Z_e^2)+[(\langle Z\rangle_{\rm av}^2-Z_e^2)/Z_e^2]u_0(\Gamma Z_e^2)\,. \tag{36}$$

We now minimize the right-hand side of (36) with respect to Z_e; using (30) this leads to the following simple equation for Z_e:

$$(Z_e^2-\langle Z\rangle_{\rm av}^2\,c_v^{(0)}(\Gamma Z_e^2)=0\,, \tag{37}$$

where $c_v^{(0)}$ is the specific heat at constant volume of the OCP; since $c_v^{(0)}>0$, the only solution of (37) is $Z_e=\langle Z\rangle_{\rm av}$. The corresponding upper bound is not very useful since the predicted free energies lie more than 5% above their exact values for $Z_2/Z_1=2$.

On the other hand the ion sphere model, which leads to the lower bound (18) for the energy, suggests the choice

$$Z_e^2=\langle Z\rangle_{\rm av}^{1/3}\,\langle Z^{5/3}\rangle_{\rm av} \tag{38}$$

for the effective charge.[22] With this choice we find, from (32) and (33), for $\Gamma'\gtrsim 1$:

$$\Delta u(\Gamma', x_1) = b\Gamma'^{1/4}[(\langle Z^{5/3}\rangle_{av})^{1/4} - \langle (Z^{5/3})^{1/4}\rangle_{av}], \quad (39)$$

$$\Delta f(\Gamma', x_1) = 4\Delta u + c(\ln\langle Z^{5/3}\rangle_{av} - \langle \ln Z^{5/3}\rangle_{av}). \quad (40)$$

In the range of validity of these formulas, Δu and Δf are both positive slowly increasing functions of Γ'; the values predicted by (39) and (40) are about an order of magnitude larger than the corresponding HNC or MC results. For $Z_2/Z_1 = 2, x_1 = 0.5$, and $\Gamma = 40$ ($\Gamma' = 45.79$), (39) predicts $\Delta u = 0.078$ and (40) $\Delta f = 0.222$. These figures, although small, are definitely larger than the statistical errors on our Monte Carlo results which predict that these quantities differ from zero by less than the combined statistical uncertainties (~0.03 for Δu). We conclude that, although the choice (38) in conjunction with the OCP equation of state yields excellent *absolute* thermodynamic properties, the small *differences* Δu and Δf, which are essential in determining the thermodynamic stability of the TCP against demixing (cf. Sec. VII), are strongly overestimated by this simple "one-fluid model."

If we assume that the free energy of the crystalline phase is obtained with a comparable accuracy when calculated in the framework of the one-fluid model with Z_e given by (38), we can estimate the coexistence curve between the fluid and solid phases of the TCP in the (Γ, x_1) plane from the known result for the OCP.[2] The curve is then simply given by

$$\Gamma'\langle Z^{5/3}\rangle_{av} = \Gamma\langle Z\rangle_{av}^{1/3}\langle Z^{5/3}\rangle_{av} \simeq 155. \quad (41)$$

VII. MISCIBILITY IN A RIGID BACKGROUND

Until now we have been concerned only with the thermodynamic properties of ionic mixtures without explicitly considering the properties of the background (i.e., the degenerate electron gas) and without investigating the possibility of phase separation (or demixing). Since the electron gas is supposed to be completely degenerate, its properties depend only on r_s, as defined by (5). In particular, if the electrons are nonrelativistic ($r_s > 10^{-2}$), their pressure P_e is given approximately by the Nozières-Pines formula[23]:

$$\frac{P_e V}{N'} = \left(\frac{1.473}{r_s^2} - \frac{0.305}{r_s} - 0.0103\right) \text{Ry}. \quad (42)$$

We have checked that the effect of finite temperature corrections on the phase diagrams, which will be presented later, is completely negligible. The total pressure of the system is the sum of ionic and electronic pressures

$$P = P_e + P_i.$$

If we investigate the possibility of phase separation at constant pressure, we must consider the Gibbs free energy of mixing

$$\Delta G = G(P, T, N', x_1) - G(P, T, N_1', x_1 = 1) - G(P, T, N_2', x_1 = 0), \quad (43)$$

where $N' = Z_1N_1 + Z_2N_2$ is the total number of charges (i.e., electrons),

$$N_1' = (Z_1x_1/\bar{Z})N' = Z_1N_1 \text{ and } N_2' = (Z_2x_2/\bar{Z})N' = Z_2N_2.$$

We first consider the simplest case where the ionic pressure is negligible compared to the electronic pressure ($P_i \ll P_e$): this corresponds to the limit $r_s \to 0$, typical of white dwarf matter (where $r_s \simeq 10^{-2}$). Since P_e is a function of r_s only, the condition of constant pressure is then equivalent to the condition of constant charge density, and ΔG coincides with ΔF, which depends now only on ionic properties:

$$\Delta G = \Delta F = F(\rho', T, N, x_1) - F(\rho', T, N_1, x_1 = 1) - F(\rho', T, N_2, x_1 = 0), \quad (44)$$

or equivalently,

$$\frac{\beta\Delta F}{N} = \frac{\beta F}{N}(\Gamma', x_1) - x_1\frac{\beta F}{N}(\Gamma', x_1 = 1) - x_2\frac{\beta F}{N}(\Gamma', x_1 = 0). \quad (45)$$

$\beta\Delta F/N$ is the sum of the *excess* part Δf, which has been calculated in the preceding sections, and of the ideal-gas part (i.e., minus the ideal entropy of mixing):

$$\frac{\beta\Delta F}{N} = \Delta f + x_1 \ln\frac{x_1 Z_1}{\langle Z\rangle_{av}} + x_2 \ln\frac{x_2 Z_2}{\langle Z\rangle_{av}}. \quad (46)$$

From our result for Δf, Eq. (31), it is clear that the TCP is miscible under all conditions in the limit $r_s \to 0$, since the excess free energy of mixing Δf is too small to compensate the ideal entropy of mixing.

However for finite values of r_s, the ionic contribution to the pressure ceases to be negligible to the electronic contribution. The condition of equal pressures for the coexisting phases leads then to different charge densities of these phases, and the calculated ΔG exhibits regions of negative curvature as a function of x_1 (for fixed P and T) which are characteristic of phase separation. These thermodynamically unstable states are eliminated by the usual double-tangent construction.

The resulting coexistence curves in the (T, x_1) plane are shown in Figs. 3 ($Z_1 = 1, Z_2 = 2$) and 4 ($Z_2 = 3$) for two values of the reduced pressure $\pi = Pa_0^4/e^2$. $\pi = 1$ corresponds to a pressure of 294.2 Mbar; a reduced pressure $\pi = 0.1$ is typical of pressures believed to exist in the deep interior of Jupiter. In

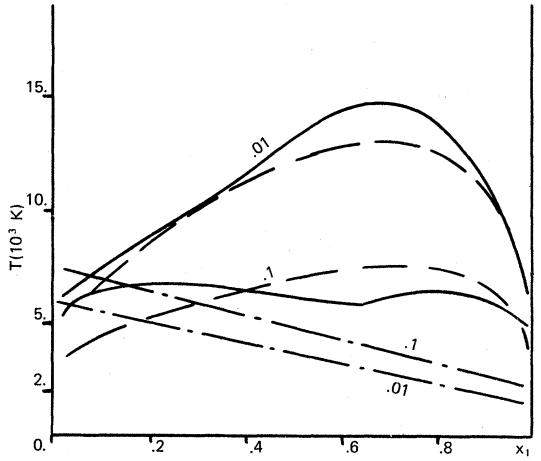

FIG. 3. Phase-separation curves for H^+-He^{++} mixtures under reduced pressures $\pi = 0.1$ (upper curves) and $\pi = 0.01$ (lower curves). The dashed curves are for a rigid background, whereas the full curves correspond to a polarized background with Lindhard screening and include ionic quantum corrections. The dash-dotted lines are estimates of the fluid-solid coexistence curves based on Eq. (1).

calculating these coexistence curves, we have used our HNC results for the free energy and the equation of state of the TCP (see Sec. IV), including the small nonadditive corrections Δu and Δf. The coexistence curves are practically unchanged upon setting $\Delta u = \Delta f = 0$, or upon replacing the HNC results by the MC data.

Inspection of Figs. 3 and 4 shows that, as expected, the critical temperature of demixing decreases with increasing pressure, since the corresponding charge density then increases, and we have seen that in the limit $r_s \to 0$, the mixture is always stable. The most striking difference between the two sets of coexistence curves is the sharp increase of the critical temperature (by almost an order of magnitude!) for a given pressure, in going from $Z_2 = 2$ to $Z_2 = 3$.

Coexistence curves for H^+-He^{++} mixtures have also been calculated by Pollock and Alder,[22] using the one-fluid model with the effective charge given by (38). The excess internal and free energies of mixing are then given by (39) and (40). The resulting (T, x_1) curves lie well above our results, indicating that the precise location of these coexistence curves depends very sensitively on Δu and Δf, which are overestimated by the one-fluid model.

Before we can compare our coexistence curves with the results of Stevenson,[5] we must include quantum corrections for the ions and electron screening corrections in our calculations. This will be done in Sec. VIII.

VIII. QUANTUM- AND ELECTRON-SCREENING CORRECTIONS

In this section we apply our results for the TCP model to a "realistic" calculation of the thermodynamics and phase diagram of H^+-He^{++} and H^+-Li^{+++} mixtures. To do so we must include two effects which are generally non-negligible in the pressure and temperature range considered here: quantum corrections to the thermodynamic properties of the ions and electron-screening corrections due to the polarization of the electron gas by the ions. Both corrections have already been considered in the case of the OCP,[24,25] and we present here the straightforward extension to the TCP.

Let $\Lambda_\nu = (h^2/2\pi M_\nu k_B T)^{1/2}$ be the de Broglie thermal wavelength of the ionic species ν of mass M_ν. We expect quantum effects to become important when

$$\frac{\Lambda_\nu}{a'} = \left(\frac{\Gamma'}{r_s}\frac{m}{2\pi M_\nu}\right)^{1/2} \simeq 1, \tag{46'}$$

where m is the electron rest mass. As long as $\Lambda_\nu/a' \ll 1$, the Wigner expansion[26] of the free energy in powers of h^2 is expected to be sufficient to account for ion quantum corrections. Limiting ourselves to the lowest-order correction ($\sim h^2$), we obtain, after a straightforward calculation, and with the help of Poisson's equation:

$$f(\Gamma', x_1, r_s) = f^{\mathrm{cl}}(\Gamma', x_1) + \frac{1}{8}\frac{\Gamma'^2}{r_s}\left(\frac{Z_1 x_1}{M_1/m} + \frac{Z_2 x_2}{M_2/m}\right), \tag{47}$$

where f^{cl} is the classical excess free energy per ion, defined by equation (24). As expected the quantum corrections break the simple scale invariance of the excess thermodynamic properties

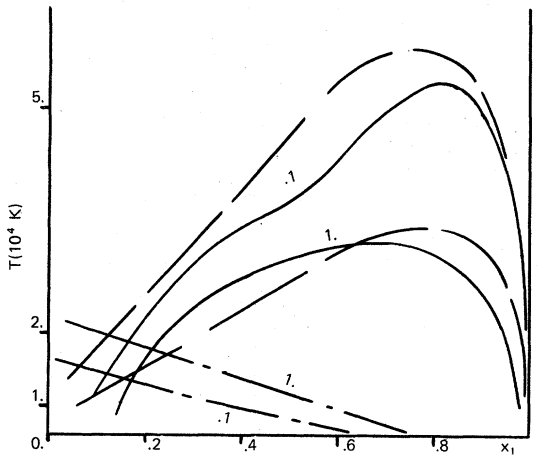

FIG. 4. Same as Fig. 3, but for H^+-Li^{+++} mixtures under reduced pressures $\pi = 0.1$ and 1.

of the classical TCP, i.e., their dependence on two, rather than three, independent variables (Γ' or Γ and x_1), through the introduction of the characteristic length (46'); the excess free energy (47) of the ions depends now on r_s, in addition to Γ' and x_1.

On the other hand the rigid uniform background approximation for the electron gas is valid only at very high density ($r_s \to 0$). At densities of astrophysical interest or in situations characteristic of laser-imposed superdense matter ($10^{-2} \lesssim r_s \lesssim 1$), the electron gas is polarized by the ionic charge distribution and the formation of polarization clouds around the ions modifies the ion-ion interaction. The importance of this effect can be characterized by the dimensionless Thomas-Fermi wave vector

$$q_{TF} = ak_{TF} = (12\langle Z\rangle_{av}/\pi)^{1/3} r_s^{1/2}. \tag{48}$$

The rigid background approximation becomes exact in the limit $q_{TF} \to 0$. Electron screening effects are expected to become important when $q_{TF} \simeq 1$.

We now follow closely the very similar calculation for the OCP.[25] Limiting ourselves to the linear response of the electron gas to the ionic charge distribution, and considering this response to be instantaneous, which is justified in view of the large mass ratios M_ν/m, we write the interaction Hamiltonian of the ions in the presence of a responding background:

$$H = \frac{1}{2V}{\sum_{\vec{k}}}' \frac{4\pi e^2}{k^2}\left[\rho'_{\vec{k}}\rho'_{-\vec{k}} - N\langle Z\rangle_{av}^2\right]$$

$$+\frac{1}{2V}\sum_{\vec{k}} \frac{4\pi e^2}{k^2}\left(\frac{1}{\epsilon(k)} - 1\right)\rho'_{\vec{k}}\rho'_{-\vec{k}} = H_0 + H_1, \tag{49}$$

where $\epsilon(k)$ is the static dielectric constant of the degenerate electron gas, H_0 is the "unperturbed" (or "reference") Hamiltonian (1), and H_1 is the "perturbation." This separation of H is justified, since $\epsilon(k) \to 1$ for all k, in the limit $r_s \to 0$, and hence H reduces to H_0 in that limit. For finite values of r_s we have treated H_1 by thermodynamic perturbation theory.[27] To first order the excess Hemholtz free energy per particle is given by

$$f(\Gamma; x_1; r_s) = f^{(0)}(\Gamma; x_1) + (1/N)\langle \beta H_1\rangle, \tag{50}$$

where $f^{(0)}$ is the free energy of the reference system, i.e., the TCP, and the statistical average is taken over the reference system canonical ensemble. In reduced units,

$$\frac{\beta\langle H_1\rangle}{N} = \frac{1}{3\pi}\int_0^\infty S'(q)\hat{w}(q)q^2\,dq, \tag{51}$$

where $S'(q)$ is the charge structure factor (10) of the reference system and $\hat{w}(q)$ is the perturbation potential, divided by $k_B T$, and averaged over ionic species:

$$\hat{w}(q) = (3\Gamma\langle Z^2\rangle_{av}/q^2)[1/\epsilon(q) - 1]. \tag{52}$$

In the following we shall limit ourselves to the first-order theory (50), which yields an upper bound to the free energy of the ionic system characterized by the Hamiltonian (49). As long as we consider situations where $r_s \lesssim 1$, we expect the higher-order terms to be small.[25]

In order to evaluate (51), we must choose an appropriate dielectric constant $\epsilon(q)$. In the high-density limit ($r_s \ll 1$), the random-phase approximation (RPA) becomes exact, and the corresponding $\epsilon(q)$ due to Lindhard[8] reads

$$\epsilon_L(q) = 1 + (q_{TF}^2/q^2) f(y),$$
$$f(y) = \tfrac{1}{2} + [(1-y^2)/4y]\ln\left|(1+y)/(1-y)\right|, \tag{53}$$

where $y = q/2q_F$ and $q_F = (9\pi\langle Z\rangle_{av}/4)^{1/3}$ is the reduced Fermi wave number.

For $r_s \simeq 1$, $\epsilon_L(q)$ must be corrected for exchange and correlation effects. Following the pioneer work of Hubbard,[6] we cast $\epsilon(q)$ in the general form

$$\epsilon(q) = 1 + \frac{q_{TF}^2}{q^2}\frac{f(y)}{1 - (q_{TF}^2/q^2)f(y)G(y)}. \tag{54}$$

The RPA is recovered with the particular choice $G(y) = 0$. Geldart and Vosko[6] suggested the form

$$G(y) = y^2/(2y^2 + g), \tag{55}$$

with $g = 1/(1 + 0.026 r_s)$ in order to satisfy the compressibility sum rule for the degenerate electron gas.[13] We shall refer to this form of $\epsilon(q)$ as the Hubbard-Geldart-Vosko (HGV) dielectric function. Note that for $r_s \lesssim 0.01$, the electron gas becomes relativistic, so that the relativistic counterpart of $\epsilon_L(q)$ must be used.[25,28]

Replacing (52) and (54) in (51) we obtain the following expression for the first-order correction to the free energy:

$$\langle \beta H_1\rangle = f^{(1)}(\Gamma; x_1; r_s)$$
$$= -\frac{\Gamma\langle Z^2\rangle_{av}}{\pi}\int_0^\infty S'(q)\left(\frac{\epsilon(q) - 1}{\epsilon(q)}\right)dq$$
$$= -\frac{\Gamma\langle Z^2\rangle_{av}}{\pi} q_{TF}^2 \int_0^\infty \frac{S'(q) f(y)}{q^2 - q_{TF}^2 f(y) H(y)}\,dq, \tag{56}$$

where $H(y) = G(y) - 1$.

Since we are mainly interested in situations where $q_{TF} \lesssim 1$, we have expanded $f^{(1)}$ in powers of q_{TF} (i.e., in powers of $r_s^{1/2}$):

$$f^{(1)}(\Gamma; x_1; r_s) = q_{TF}^2[A(\Gamma, x_1) + \tfrac{1}{6} q_{TF} + C(\Gamma, x_1) q_{TF}^2$$
$$+ D(\Gamma, x_1) q_{TF}^3 + O(q_{TF}^4)], \tag{57}$$

where the coefficients A, C, and D are given ex-

TABLE IV. Electron-screening corrections to the excess Helmholtz free energy of H^+-He^{++} mixtures at $r_s = 0.8$. $f^{(0)}$ is the free energy in a rigid background; $f_L^{(1)}$ and $f_H^{(1)}$ are the first-order screening corrections using the Lindhard and HGV dielectric functions. Our data are based on the HNC results; the MC data are those of DeWitt and Hubbard (Ref. 7).

	$x_2=\frac{1}{6}$			$x_2=\frac{1}{2}$		
Γ	$f^{(0)}$	$f_L^{(1)}$	$f_L^{(1)}$ (MC)	$f^{(0)}$	$f_L^{(1)}$	$f_H^{(1)}$
5	−5.193	−0.949	−0.785	−8.687	−1.683	−1.696
10	−11.254	−1.518	−1.366	−18.532	−2.837	−2.905
20	−23.837	−2.557	−2.427	−38.800	−5.048	−5.208
40	−49.634	−4.541	−4.433	−80.106	−9.385	−9.706
60	−75.774	−6.484	−6.381	−121.84	−13.69	−14.16

plicitly in Appendix B. In practice the expansion turns out to converge surprisingly well up to $q_{TF} \simeq 2$ for $\Gamma > 1$. The dominant term is seen to be *linear* in r_s, in agreement with the Monte Carlo results of De Witt and Hubbard.[7] Note that the coefficients of the two lowest-order terms [$A(\Gamma, x_1)$ and $\frac{1}{6}$] are in fact independent of the function $G(y)$, so that the values obtained for $f^{(1)}$ turn out to be rather insensitive to the choice of $\epsilon(q)$.

We have calculated $f^{(1)}$ and the coefficients, A, C, and D using our HNC results for the TCP charge structure factor. Our results for A, C, and D have been fitted by simple functions of Γ, for fixed values of x_1, and these are given in Appendix B. Some numerical examples at $r_s = 0.8$ are given in Table IV for H^+-He^{++} mixtures, and a comparison is made with the Monte Carlo results obtained by De Witt and Hubbard[7] for $x_2 = \frac{1}{6}$ (the highest He concentration considered by these authors), using Lindhard screening. The agreement between their and our $f^{(1)}$ values is satisfactory considering the rather large numerical uncertainties on the MC data of these authors. The table also confronts the free energies which we have calculated using the Lindhard and HGV dielectric functions at $r_s = 0.8$ and $x_2 = 0.5$.

It is worthwhile mentioning that, for fixed values of the charge density, and temperature (i.e., r_s and Γ'), $f^{(1)}$ is nearly additive, exactly as $f^{(0)}$, both for H^+-He^{++} and H^+-Li^{+++} mixtures:

$$f^{(1)}(\Gamma'; x_1; r_s) \simeq x_1 f^{(1)}(\Gamma'; x_1 = 1; r_s) + x_2 f^{(1)}(\Gamma'; x_2 = 1; r_s). \quad (58)$$

However, the small nonadditive contribution $\Delta f^{(1)}$ turns out to be crucial in the accurate determination of phase diagrams.

We have recalculated the H^+-He^{++} and H^+-Li^{+++} coexistence curves, including the lowest-order quantum correction (47) and electron screening correction (56). The various contributions to the Gibbs free energy of mixing are shown for a typical case in Fig. 5, as a function of x_1. The contributions to ΔG from electron screening are nearly identical when calculated with the Lindhard or HGV dielectric functions; the corresponding coexistence curves are very close and we present in Figs. 3 and 4 the results obtained with the Lindhard dielectric function at two reduced pressures. From the figures it is immediately apparent that the quantum and screening corrections do not drastically modify the coexistence curves obtained in Sec. VII for purely *classical* ions in a *rigid* background.

At $\pi = 0.1$, the H^+-He^{++} coexistence curve exhibits two maxima, i.e., two critical points separated by a minimum. This feature is due to the screening corrections and persists at higher pressures, but disappears towards lower pressures where the two maxima merge into one. No similar feature is observed for H^+-Li^{+++} mixtures. We must stress however that the calculated coexistence curves are very sensitive to small numerical inaccuracies on ΔG. The precise location of the critical point and the existence of the double maximum could very well be considerably affected by higher-order screening corrections. However, the explicit calculation of such terms requires approximations leading to uncertainties which are of the same order of magnitude as the corrections themselves; consequently we have not included higher-order corrections in our calculations.

In Fig. 6 we compare our coexistence curve with the results of Stevenson[5] for a H^+-He^{++} mixture at $\pi = 0.1$. Our results obtained with the Lindhard and HGV dielectric functions are nearly undistinguishable on the scale of the figure. Stevensen used the HGV dielectric function and added corrections for the nonlinear response of the electron gas to the ionic charge distribution; he predicts a somewhat higher critical temperature, but the overall agreement between his and our results is satisfactory, considering the very different approaches.

Finally, in Table V, we list the critical temperatures and concentrations, as a function of π, both for H^+-He^{++} and H^+-Li^{+++} mixtures.

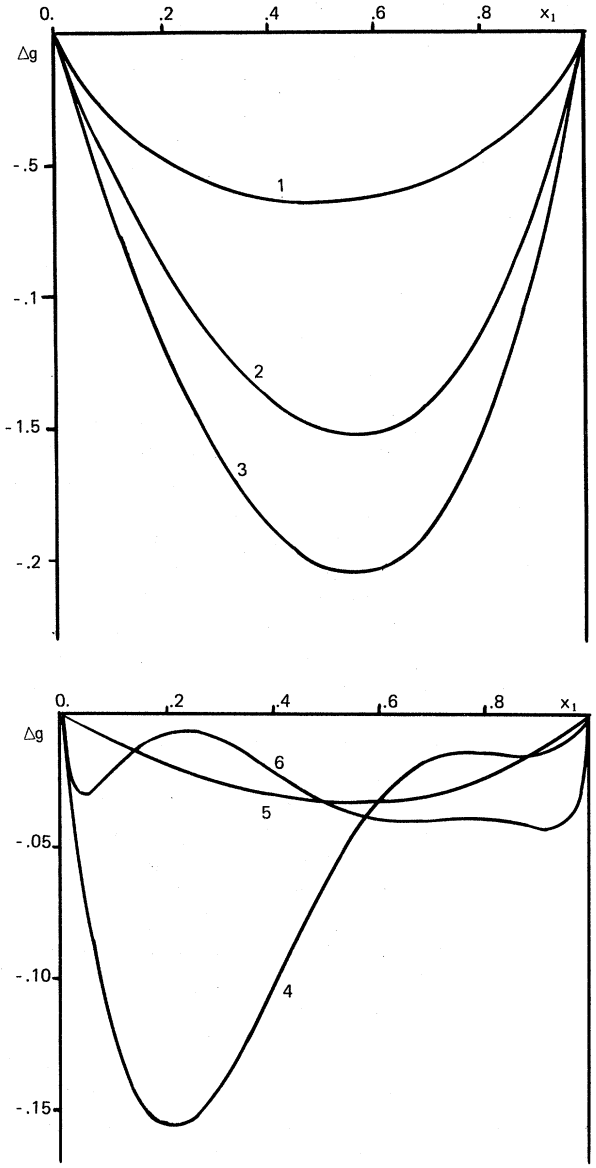

FIG. 5. Contributions to the Gibbs free energy of mixing $\beta\Delta G/N$ for a H^+-He^{++} mixture under a reduced pressure $\pi = 0.1$ and $T = 5850$ K. (1) Ideal entropy of mixing; (2) electronic contribution [cf. Eq. (42)]; (3) *minus* the ionic excess contribution in a rigid background; (4) *minus* the screening correction, using the Lindhard $\epsilon(k)$; (5) h^2 quantum correction to the ionic contribution; (6) sum of all five contributions.

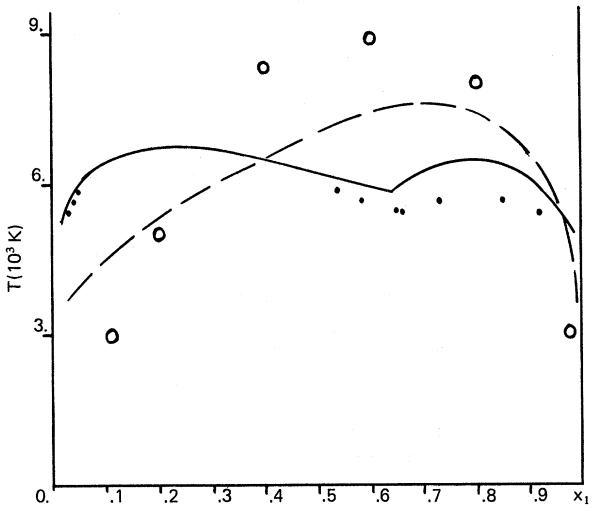

FIG. 6. Comparison between H^+-He^{++} phase-separation curves for a reduced pressure $\pi = 0.1$ (29.4 Mbar) under the following conditions: dashed curve, rigid background; full curve, polarized background with Lindhard screening; dots, Hubbard-Geldart-Vosko screening (only a few points are indicated); circles, results of Stevenson (Ref. 5) using the latter dielectric constant.

IX. CONCLUSIONS

We have considered in some detail a simple model of two species of point ions in a uniform background. If this background is assumed to be rigid, the main result of our accurate numerical calculations is that the excess thermodynamic properties

TABLE V. Variation of critical temperature, density (r_s), and concentration with reduced pressure $\pi = Pa_0^4/e^2$ ($\pi = 1$ corresponds to a pressure of 294.2 Mbar) for ionic mixtures with $Z_1 = 1$, $Z_2 = 2$ and 3, using Lindhard screening. In the case $Z_2 = 2$, we have indicated the critical parameters corresponding to the two maxima in the coexistence curve which appear for $\pi \gtrsim 0.1$.

π	T (10^3 K)	x_1	r_s
	$Z_1 = 1$; $Z_2 = 2$		
0.01	14.75	0.69	1.277
0.02	11.04	0.675	1.150
0.05	7.55	0.745	1.021
0.1	6.44	0.795	0.926
0.2	5.91	0.815	0.832
0.5	5.54	0.835	0.716
1	5.39	0.84	0.635
2	5.32	0.84	0.562
0.1	6.75	0.23	0.878
0.2	6.75	0.21	0.795
0.5	6.83	0.19	0.689
1	6.95	0.18	0.615
2	7.08	0.175	0.547
	$Z_1 = 1$; $Z_2 = 3$		
0.05	5.44	0.82	1.095
0.1	5.35	0.82	0.964
0.2	4.71	0.815	0.842
0.5	3.63	0.75	0.703
1	3.22	0.70	0.619

are very nearly additive at constant Γ', i.e., the excess properties of mixing $(\Delta u, \Delta f, \Delta G)$ represent a practically negligible fraction of the excess properties of the mixture and of the pure phases. There is no obvious physical explanation for this striking feature. The only hint towards an understanding of the additivity is the fact that the lower bound (18) for the internal energy satisfies the property exactly; for large values of Γ' the internal energy of the mixture, derived from our HNC or MC calculations, lies within a few percent of this bound.

The near additivity of the thermodynamic properties of the mixture at constant Γ' allows us to express these in terms of the properties of the one-component plasma which are known very accurately. We used the corresponding equation of state to study the coexistence curves of H^+-He^{++} and H^+-Li^{+++} mixtures in a rigid and in a responding electron background. The first case is a good approximation in the high-density limit ($r_s \ll 1$), typical of degenerate stellar matter (white dwarfs). Our results clearly indicate that under such extreme conditions ionic mixtures are always stable against demixing. At lower densities ($0.5 \lesssim r_s \lesssim 1$), typical of the interior of Jupiter, the situation is less simple, because electron screening effects become important. In fact in the corresponding pressure range ($P \simeq 50$ Mbar), hydrogen is completely ionized, but helium may very well not be pressure ionized.[22] Our calculations, which assume complete ionization of both ionic species, show that the electron screening effects, treated to lowest order, do not appreciably modify the coexistence curves, and in particular the critical temperature, as compared to the rigid background case. The values we have obtained for the critical temperatures are very sensitive to small changes in the excess Gibbs free energy of mixing ΔG, especially to the electron-screening contribution to ΔG. In particular the existence of a double maximum in the H^+-He^{++} coexistence curves at high pressures must be accepted with caution, since higher-order electron-screening corrections may very well change ΔG sufficiently to suppress this feature.

Finally we would like to point out that our results can be applied to cases where one (or both) ionic species are only partially ionized (e.g., Li^+), provided Γ is sufficiently large so that the remaining ion core is of smaller radius than the distance of closest approach, which is essentially determined by the range of interionic distances r over which the pair-distribution functions $g_{\nu\mu}(r)$ are practically zero.

TABLE VI. Coefficients a_1, a_2, and a_3 in Eq. (B5) as a function of concentration for H^+-He^{++} and H^+-Li^{+++} mixtures.

x_1	$a_1(x_1)$	$a_2(x_1)$	$a_3(x_1)$
	$Z_1=1;\ Z_2=2$		
0	−0.142548	−0.40086	0.08151
0.25	−0.116518	−0.38382	0.08611
0.50	−0.088105	−0.36582	0.09376
0.75	−0.056562	−0.34315	0.10282
1	−0.019573	−0.33073	0.13331
	$Z_1=1;\ Z_2=3$		
0	−0.388602	−0.49450	0.08339
0.25	−0.316052	−0.45826	0.08229
0.5	−0.244867	−0.42056	0.08537
0.75	−0.141028	−0.36722	0.08490
1	−0.019573	−0.33073	0.13331

ACKNOWLEDGMENTS

We are indebted to Hugh De Witt for useful correspondence and to Jean-Jacques Weis for his help in preparing an efficient HNC program. One of us (G.M.T.) wishes to thank the Laboratoire de Physique Théorique, Orsay (France) for their kind hospitality and use of their computing facilities, and gratefully acknowledges financial support in the form of a postdoctoral fellowship from the National Research Council of Canada.

APPENDIX A

In this appendix we prove Eq. (25) valid in the framework of HNC theory. Let $z_\nu = e^{\beta\mu_\nu}/(\rho_\nu \Lambda_\nu^3)$ be the activities of the two ionic species; Λ_ν is the thermal de Broglie wavelength for species ν; then $\beta\mu_\nu^{ex} = \ln z_\nu$ is given by the exact relation[29]

$$\ln z_\nu = \rho \int_0^1 d\lambda \int d\vec{r} \sum_{\mu=1}^{2} x_\mu \beta v_{\nu\mu}(r) h_{\nu\mu}(r;\lambda), \qquad \text{(A1)}$$

where $h_{\nu\mu}(r;\lambda)$ is the pair-correlation function between a single ion of species ν which interacts with the ions of species μ via the potential $\lambda v_{\nu\mu}(r)$, $0 \le \lambda \le 1$. Note that $h_{\nu\mu}$ replaces here the usual $g_{\nu\mu}$ to account for the background interaction. If we define the function $\gamma_{\nu\mu}(r;\lambda)$ through

$$h_{\nu\mu}(r;\lambda) = \exp[-\beta\lambda v_{\nu\mu}(r) + \gamma_{\nu\mu}(r;\lambda)] - 1, \qquad \text{(A2)}$$

we obtain upon differentiation with respect to λ:

$$\beta v_{\nu\mu}(r) h_{\nu\mu}(r;\lambda) = -\frac{\partial}{\partial\lambda} h_{\nu\mu}(r;\lambda) + \frac{\partial}{\partial\lambda} \gamma_{\nu\mu}(r;\lambda) - \beta v_{\nu\mu}(r) + \frac{\partial}{\partial\lambda} \gamma_{\nu\mu}(r;\lambda)\, h_{\nu\mu}(r;\lambda), \qquad \text{(A3)}$$

upon replacing (A3) in (A1), we can immediately perform the integration over λ for the first three terms on the right-hand side of (A3) and we are

left with the exact relation

$$\ln z_\nu = \rho \int d\vec{r} \sum_{\mu=1}^{2} x_\mu [\gamma_{\nu\mu}(r) - h_{\nu\mu}(r) - \beta v_{\nu\mu}(r)] + \rho \int_0^1 d\lambda \int d\vec{r} \sum_{\mu=1}^{2} x_\mu h_{\nu\mu}(r;\lambda) \frac{\partial}{\partial\lambda} \gamma_{\nu\mu}(r;\lambda), \tag{A4}$$

where $h_{\nu\mu}(r) \equiv h_{\nu\mu}(r;\lambda=1)$ and $\gamma_{\nu\mu}(r) \equiv \gamma_{\nu\mu}(r;\lambda=1)$. The second term on the right-hand side of (A4) can also be integrated over λ if we make the HNC approximation (23), according to which

$$\gamma_{\nu\mu}(r;\lambda) = h_{\nu\mu}(r;\lambda) - c_{\nu\mu}(r;\lambda), \tag{A5}$$

where use was made of (22) and (A2). If $\hat{h}_{\nu\mu}$ and $\hat{\gamma}_{\nu\mu}$ are the Fourier transform of $h_{\nu\mu}$ and $\gamma_{\nu\mu}$, we have the following Ornstein-Zernike relation [cf. (7)]:

$$\hat{\gamma}_{\nu\mu}(k;\lambda) = \sum_\alpha x_\alpha \hat{h}_{\nu\alpha}(k;\lambda)[\hat{h}_{\alpha\mu}(k) - \hat{\gamma}_{\alpha\mu}(k)]. \tag{A6}$$

The second term on the right-hand side of (A4) then becomes, upon using Parseval's theorem and (A6):

$$\rho \int_0^1 d\lambda \int d\vec{k} \sum_\mu x_\mu \hat{h}_{\nu\mu}(k;\lambda) \frac{\partial}{\partial\lambda} \hat{\gamma}_{\nu\mu}(k;\lambda) = \frac{\rho}{2} \int d\vec{k} \int_0^1 d\lambda \sum_\mu \sum_\alpha x_\mu x_\alpha \frac{\partial}{\partial\lambda} [\hat{h}_{\nu\mu}(k;\lambda)\hat{h}_{\nu\alpha}(k;\lambda)][\hat{h}_{\alpha\mu}(k) - \hat{\gamma}_{\alpha\mu}(k)]$$
$$= \frac{\rho}{2} \int d\vec{k} \sum_\mu \hat{h}_{\mu\nu}(k) \sum_\alpha x_\alpha \hat{h}_{\nu\alpha}(k)[\hat{h}_{\alpha\mu}(k) - \hat{\gamma}_{\alpha\mu}(k)]$$
$$= \frac{\rho}{2} \int d\vec{r} \sum_\mu h_{\nu\mu}(r)\gamma_{\nu\mu}(r).$$

Gathering results and returning to reduced units ($x = r/a$ and $\rho a^3 = 3/4\pi$), we recover Eq. (25).

APPENDIX B

The first-order electron-screening correction to the Helmholtz free energy of the TCP, given by Eq. (56), can be expanded in powers of the reduced Thomas-Fermi wave number q_{TF}, defined by (48). A straightforward calculation yields for the coefficients A, C, and D in Eq. (57):

$$A(\Gamma;x_1) = -\frac{\Gamma\langle Z^2\rangle_{av}}{\pi} \frac{1}{2q_F} \int_0^\infty dy \frac{S'(y)f(y)}{y^2}, \tag{B1}$$

$$C(\Gamma;x_1) = -\frac{\Gamma\langle Z^2\rangle_{av}}{\pi} \frac{1}{8q_F^3} \int_0^\infty dy \frac{1}{y^4} \times \left(S'(y)f^2(y)H(y) + \frac{4q_F^2}{3\Gamma\langle Z^2\rangle_{av}} y^2 \right), \tag{B2}$$

$$D(\Gamma;x_1) = (1/48q_F^2)(\tfrac{5}{3} + 3/g - 8q_F^2\delta), \tag{B3}$$

where δ is defined in Eq. (14), and g was introduced in Eq. (55); $1/g = 0$ (1) for the Lindhard (HGV) dielectric function; $S'(q)$ is the charge structure factor of the TCP. If we neglect the very small excess free energy of mixing Δf [cf. Eq. (31)], expression (14) for δ simplifies to

TABLE VII. Coefficients c_1, c_2, and c_3 of $C(\Gamma;x_1)$ in Eq. (B5), as a function of concentration for H^+-He^{++} and H^+-Li^{+++} mixtures, and for the Lindhard and HGV dielectric functions.

	Lindhard			HGV		
x_1	$c_1(x_1)$	$c_2(x_1)$	$c_3(x_1)$	$c_1(x_1)$	$c_2(x_1)$	$c_3(x_1)$
			$Z_1=1;\ Z_2=2$			
0	0.001604	0.15438	−0.20143	0.000292	0.14175	−0.19997
0.25	0.003063	0.11331	−0.15311	0.001888	0.10064	−0.15179
0.5	0.002634	0.11916	−0.16981	0.001665	0.10639	−0.16846
0.75	0.001882	0.11834	−0.18269	0.001232	0.10571	−0.18143
1	−0.00394	0.10544	−0.20127	−0.000484	0.09348	−0.20020
			$Z_1=1;\ Z_2=3$			
0	0.007218	0.19204	−0.20176	0.003528	0.17929	−0.20030
0.25	0.006976	0.19153	−0.20477	0.003562	0.17841	−0.20324
0.5	0.010359	0.14761	−0.16958	0.007382	0.13422	−0.16808
0.75	0.008041	0.16151	−0.20293	0.005898	0.14802	−0.20140
1	−0.000394	0.10544	−0.20127	−0.000484	0.09348	−0.20020

TABLE VIII. Coefficients d_1–d_5 in Eq. (B6), as a function of concentration for H^+-He^{+++} and H^+-Li^{+++} mixtures.

x_1	d_1	d_2	d_3	d_4	d_5
			$Z_1=1;\ Z_2=2$		
0	-0.29538×10^{-2}	0.36762×10^{-1}	0.55775×10^{-1}	0.103398	−0.143098
0.25	-0.37034×10^{-3}	0.19893×10^{-1}	0.138702	-0.84515×10^{-2}	−0.106490
0.5	0.19607×10^{-2}	0.76733×10^{-2}	0.198421	-0.73436×10^{-1}	−0.122229
0.75	0.23228×10^{-2}	0.17191×10^{-1}	0.159741	-0.28266×10^{-1}	−0.190719
1	-0.73845×10^{-3}	0.18381×10^{-1}	0.55775×10^{-1}	0.206791	−0.572391
			$Z_1=1;\ Z_2=3$		
0	-0.66461×10^{-2}	0.55143×10^{-1}	0.55775×10^{-1}	0.68932×10^{-1}	-0.63599×10^{-1}
0.25	0.69752×10^{-3}	0.15960×10^{-1}	0.184669	-0.40724×10^{-1}	-0.43747×10^{-1}
0.5	0.54191×10^{-2}	0.12569×10^{-1}	0.219740	-0.56575×10^{-1}	-0.60028×10^{-1}
0.75	0.10614×10^{-1}	0.17276×10^{-1}	0.236936	-0.63926×10^{-1}	−0.103284
1	-0.73845×10^{-3}	0.18381×10^{-1}	0.55775×10^{-1}	0.206796	−0.572391

$$\delta \simeq -\frac{1}{3\Gamma\langle Z\rangle_{\rm av}}\left\{\beta\left(\frac{\partial P}{\partial \rho'}\right)_{x_1,T} - \frac{\langle Z\rangle_{\rm av}^3}{\langle Z^2\rangle_{\rm av}} x_1 x_2 \times\left[\frac{\beta}{\rho'}\left(\frac{\partial P}{\partial x_1}\right)_{\rho',T}\right]^2\right\}. \tag{B4}$$

The derivatives of P with respect to ρ' and x_1 are expressible in terms of the partial inverse compressibilities $(\partial P/\partial\rho_1)_{\rho_2,T}$ and $(\partial P/\partial\rho_2)_{\rho_1,T}$; to be consistent, we have calculated these from the $q\to 0$ limits of the $\hat{c}_{\nu\mu}(q)$ [cf. Eq. (15)], rather than by differentiating the equation of state based on our HNC results. From (B1) we see that A is independent of $G(y)$, i.e., A is the same for the Lindhard, HGV, or any other dielectric function which incorporates the correct RPA high-density limit. C and D, on the other hand, depend on the chosen dielectric function. For practical use we have fitted the calculated values of A, C, and D by simple functions of Γ for different concentrations. For $\Gamma \gtrsim 1$, we have represented A by

$$A(\Gamma, x_1) = a_1(x_1)\Gamma + a_2(x_1)\Gamma^{1/4} + a_3(x_1), \tag{B5}$$

and we have used a similar function for C, with coefficients c_1, c_2, and c_3. These coefficients are listed in Tables VI and VII for $Z_1=1$, $Z_2=2$ and 3, and various concentrations. Finally we have represented the coefficient δ in D by

$$\delta = d_1(x_1)\Gamma + d_2(x_1)\Gamma^{1/2} + d_3(x_1) + d_4(x_1)\Gamma^{-1/2} + d_5(x_1)\Gamma^{-1}; \tag{B6}$$

the coefficients d_j are given in Table VIII. For concentrations not listed in the tables, A, C, and δ are obtained with sufficient accuracy by a Lagrange interpolation formula.

*Equipe associée au CNRS.
†Present address: Lash Miller Chemical Laboratories, University of Toronto (Ontario), Canada.
‡Laboratoire associé au CNRS.

[1]S. G. Brush, H. L. Sahlin, and E. Teller, J. Chem. Phys. 45, 2102 (1966).
[2](a) J. P. Hansen, Phys. Rev. A 8, 3096 (1973); (b) E. L. Pollock and J. P. Hansen, *ibid.* 8, 3110 (1973).
[3]J. P. Hansen, I. R. McDonald, and E. L. Pollock, Phys. Rev. A 11, 1025 (1975).
[4]J. F. Springer, M. A. Pokrant, and F. A. Stevens, J. Chem. Phys. 58, 4863 (1973); K. C. Ng, *ibid.* 61, 2680 (1974).
[5]D. J. Stevenson, Phys. Rev. B 12, 3999 (1975).
[6]J. Hubbard, Proc. R. Soc. Lond. A 243, 336 (1957); D. J. W. Geldart and S. H. Vosko, Can. J. Phys. 44, 2137 (1966).
[7]H. E. De Witt and W. B. Hubbard, Astrophys. J. 205, 295 (1976).
[8]J. Lindhard, K. Dan. Vidensk. Selsk. Mat.-Fys. Medd. 28, No. 8 (1954).
[9]J. P. Hansen and P. Vieillefosse, Phys. Rev. Lett. 37, 391 (1976).
[10]F. H. Stillinger and R. Lovett, J. Chem. Phys. 49, 1991 (1968).
[11]P. Vieillefosse and J. P. Hansen, Phys. Rev. A 12, 1106 (1975).
[12]P. Vieillefosse, J. Phys. Lett. (Paris) 38, L-43 (1977).
[13]D. Pines and P. Nozières, *The Theory of Quantum Liquids* (Benjamin, New York, 1966).
[14]N. D. Mermin, Phys. Rev. 171, 272 (1968).
[15]E. E. Salpeter, Australian J. Phys. 7, 353 (1954); H. E. De Witt, H. C. Graboske, and M. S. Cooper, Astrophys. J. 181, 439 (1973).
[16]E. H. Lieb and H. Narnhofer, J. Stat. Phys. 12, 291 (1975).
[17]F. J. Dyson, Ann. Phys. (N.Y.) 63, 1 (1971).
[18]H. E. De Witt, Phys. Rev. A 14, 1290 (1976).
[19]See, e.g., J. P. Hansen and I. R. McDonald, *Theory of Simple Liquids* (Academic, London, 1976), Chap. 5.

[20]L. Verlet and D. Levesque, Physica (Utr.) 28, 1124 (1962).
[21]See, e.g., Chap. 6 of Ref. 19.
[22]H. E. De Witt (private communication); E. L. Pollock and B. J. Alder, Phys. Rev. A 15, 1263 (1977).
[23]P. Nozières and D. Pines, Phys. Rev. 111, 442 (1958).
[24]J. P. Hansen and P. Vieillefosse, Phys. Lett. 53A, 187 (1975).
[25]S. Galam and J. P. Hansen, Phys. Rev. A 14, 816 (1976).
[26]E. Wigner, Phys. Rev. 40, 749 (1932).
[27]R. W. Zwanzig, J. Chem. Phys. 22, 1420 (1954).
[28]B. Jancovici, Nuovo Cimento 25, 428 (1962).
[29]See, e.g., T. L. Hill, *Statistical Mechanics* (McGraw-Hill, New York, 1956).